The crystal structure of bartelkeite, with a revised chemical formula, PbFeGe^{VI}(Ge$_2^{IV}$O$_7$)(OH)$_2 \cdot$H$_2$O, isotypic with high-pressure $P2_1/m$ lawsonite

MARCUS J. ORIGLIERI,[1] HEXIONG YANG,[1,*] ROBERT T. DOWNS,[1] ESTHER S. POSNER,[1]
KENNETH J. DOMANIK,[2] AND WILLIAM W. PINCH[3]

[1]Department of Geosciences, University of Arizona, Tucson, Arizona 85721-0077 U.S.A.
[2]Lunar and Planetary Laboratory, University of Arizona, Tucson, Arizona 85721-0092 U.S.A.
[3]19 Stonebridge Lane, Pittsford, New York 14534, U.S.A.

ABSTRACT

Bartelkeite from Tsumeb, Namibia, was originally described by Keller et al. (1981) with the chemical formula PbFeGe$_3$O$_8$. By means of electron microprobe analysis, single-crystal X-ray diffraction, and Raman spectroscopy, we examined this mineral from the type locality. Our results show that bartelkeite is monoclinic with space group $P2_1/m$, unit-cell parameters $a = 5.8279(2)$, $b = 13.6150(4)$, $c = 6.3097(2)$ Å, $\beta = 127.314(2)°$, and a revised ideal chemical formula PbFeGe^{VI}Ge$_2^{IV}$O$_7$(OH)$_2 \cdot$H$_2$O ($Z = 2$). Most remarkably, bartelkeite is isostructural with the high-pressure $P2_1/m$ phase of lawsonite, CaAl$_2$Si$_2$O$_7$(OH)$\cdot$H$_2$O, which is only stable above 8.6 GPa and a potential host for H$_2$O in subducting slabs. Its structure consists of single chains of edge-sharing FeO$_6$ and Ge1O$_6$ octahedra parallel to the c-axis, cross-linked by Ge2$_2$O$_7$ tetrahedral dimers. The average <Ge-O> bond lengths for the GeO$_6$ and GeO$_4$ polyhedra are 1.889 and 1.744 Å, respectively. The Pb atoms and H$_2$O groups occupy large cavities within the framework. The hydrogen bonding scheme in bartelkeite is similar to that in lawsonite. Bartelkeite represents the first known mineral containing both 4- and 6-coordinated Ge atoms and may serve as an excellent analog for further exploration of the temperature-pressure-composition space of lawsonite.

Keywords: Bartelkeite, germanate, hydrous mineral, crystal structure, X-ray diffraction, Raman spectra

INTRODUCTION

Germanate materials are used as analogues of silicate phases because they can be studied at attainable experimental conditions and provide an understanding of the physical and chemical properties of minerals and melts in the Earth's interior (e.g., Ringwood, and Seabrook 1963; Ross et al. 1986; Hazen et al. 1996; Henderson and Wang 2002; Iezzi et al. 2005; Nestola et al. 2008). Yet, little attention has been devoted to the Ge-analogues of *hydrous* silicates thus far (Thomas et al. 2008), despite their presumed role in the hydrogen budget of the earth (e.g., Ringwood and Major 1967; Thompson 1992; Frost 2006). Only a few high-pressure hydrous germanates in the Al$_2$O$_3$-GeO$_2$-H$_2$O system have been examined as analogs for phases in the Al$_2$O$_3$-SiO$_2$-H$_2$O system in deeply subducted rocks, where lawsonite and related phases undergo phase transformations (e.g., Schmidt 1995; Wunder and Marler 1997).

While it appears that the number of synthetic germanates has been increasing continuously, there are only 3 anhydrous and 10 hydrous natural germanates in the current list of IMA approved minerals. Unfortunately, until now, seven of these germanate minerals have not been structurally characterized, making it difficult to take full advantage of natural germanates as models of silicates at mantle conditions.

The germanate, bartelkeite, was originally described by

Keller et al. (1981) as a new mineral from Tsumeb, Namibia, with chemical formula PbFeGe$_3$O$_8$, and monoclinic symmetry with space group $P2_1$ or $P2_1/m$, unit-cell parameters $a = 5.431(3)$, $b = 13.689(7)$, $c = 5.892(3)$ Å, $\beta = 111.79(4)°$, $Z = 2$. Since then, no further study has been reported for this mineral. Here, we present the first structure solution of bartelkeite from single-crystal X-ray-diffraction data, demonstrating that its ideal chemical formula is PbFeGe$_3$O$_7$(OH)$_2 \cdot$H$_2$O, rather than PbFeGe$_3$O$_8$. Furthermore, we reveal that bartelkeite is isostructural with the high-pressure $P2_1/m$ phase of rock-forming lawsonite, CaAl$_2$Si$_2$O$_7$(OH)$\cdot$H$_2$O, which is only stable above 8.6 GPa, opening a new channel for investigating the complex phase transitions in lawsonite.

EXPERIMENTAL PROCEDURES

The bartelkeite specimen used for the study is from the type locality, Tsumeb, Namibia, and in the collection of the RRUFF Project (http://rruff.info/R070114). Its chemical composition was determined using a Cameca SX-100 electron microprobe at 25 kV and 40 nA with a beam size of 10 μm. The average of 18 analysis points gives (wt%) PbO = 34.1(2), FeO = 10.6(1), GeO$_2$ = 46.2(2), As$_2$O$_5$ = 2.8(3), SiO$_2$ = 0.10(1), ZnO = 0.08(2), P$_2$O$_5$ = 0.04(1), Cl = 0.20(6), SO$_3$ = 0.14(4), and total = 94.4(2). The chemical formula was calculated on the basis of 10 (O + Cl) atoms per formula unit, as determined from the structure refinement (see below), by adding 5.64 wt% H$_2$O to achieve charge balance, yielding Pb$_{0.97}$(Fe$^{2+}_{0.94}$Zn$_{0.01}$)$_{\Sigma=0.95}$ Ge$^{VI}_{1.00}$ (Ge$_{1.81}$As$_{0.16}$Si$_{0.01}$S$_{0.01}$)$^{IV}_{\Sigma=1.99}$O$_7$[(OH)$_{1.94}$Cl$_{0.04}$]$_{\Sigma=1.98} \cdot$1.02H$_2$O, which can be simplified as PbFeGe^{VI}Ge$_2^{IV}$O$_7$(OH)$_2 \cdot$H$_2$O.

Single-crystal X-ray diffraction data of bartelkeite were collected from a nearly equi-dimensional crystal (~0.09 × 0.09 × 0.08 mm) on a Bruker X8 APEX2 CCD X-ray diffractometer equipped with graphite-monochromatized MoKα radiation.

Reflections with $I > 2\sigma(I)$ were indexed based on a monoclinic unit cell (Table 1). To facilitate a direct comparison with the high-pressure $P2_1/m$ structure of lawsonite (Pawley and Allan 2001), we adopted in this study a unit-cell setting (setting II in Table 1) differing from the one (setting I in Table 1) given by Keller et al. (1981). The matrix for the transformation from setting I to II is (0 0 –1/0 1 0/1 0 1). No satellite or super-lattice reflections were observed. The intensity data were corrected for X-ray absorption using the Bruker program SADABS. The systematic absences of reflections suggest possible space group $P2_1$ or $P2_1/m$. The crystal structure was solved and refined using SHELX97 (Sheldrick 2008) based on the space group $P2_1/m$, because it yielded a better refinement in terms of bond lengths and angles, atomic displacement parameters, and R factors. The positions of all atoms were refined with anisotropic displacement parameters, except for H atoms, which were refined with a fixed isotropic displacement parameter (U_{iso} = 0.03). During the structure refinements, ideal chemistry was assumed, as the overall effects of the trace amounts of other elements (Zn, As, Si, S, and Cl) on the final refined structure are negligible. Final refined atomic coordinates and displacement parameters are listed in Table 2 and selected bond lengths and angles in Table 3. A CIF is available[1].

The Raman spectrum of bartelkeite was recorded on a randomly oriented crystal from 12 scans at 30 s and 200 mW power per scan on a Thermo-Almega microRaman system, using a solid-state laser with a wavelength of 532 nm and a thermoelectrically cooled CCD detector. The laser is partially polarized with 4 cm^{-1} resolution and a spot size of 1 μm.

RESULTS AND DISCUSSION

Crystal structure

Most strikingly, bartelkeite is isostructural with the high-pressure $P2_1/m$ phase of lawsonite (Pawley and Allan 2001). Its structure consists of single chains of edge-sharing FeO_6 and $Ge1O_6$ octahedra parallel to the *c*-axis, cross-linked by Ge_2O_7 tetrahedral dimers. The Pb atoms and H_2O groups occupy large cavities within the framework (Fig. 1). In fact, bartelkeite is the first known mineral containing both 4- and 6-coordinated Ge atoms. Compared to the $Ge1O_6$ octahedron, the FeO_6 octahedron is markedly distorted, as measured by the octahedral angle variance (OAV) and quadratic elongation (OQE) (Robinson et al. 1971). The OAV and OQE indexes are 136.4 and 1.042, respectively, for the FeO_6 octahedron, but only 11.4 and 1.004 for the $Ge1O_6$ octahedron. The pronounced distortion of the FeO_6 octahedron stems primarily from its edge-sharing with the smaller, more strongly bonded $Ge1O_6$ octahedron. To maintain such a linkage, the shared edges of the comparatively large and soft FeO_6 octahedron have to be shortened substantially to match those of the rigid GeO_6 octahedron, making the O-Fe-O angle subtending the shared edge (70.96°) deviate considerably from the ideal value of 90°. This is similar to the high-pressure $P2/n$ $Na(Mg_{0.5}Si_{0.5})SiO_3$ clinopyroxene, where MgO_6 and SiO_6 octahedra also share

TABLE 1. Summary of crystal data and refinement results for bartelkeite

	Bartelkeite (this study)		Bartelkeite (Keller et al. 1981)
	(setting I)	(setting II)	
Ideal chemical formula	$PbFeGe_3O_7(OH)2\cdot H_2O$		$PbFeGe_3O_8$
Space group	$P2_1/m$		$P2_1$ or $P2_1/m$
a (Å)	5.4033(2)	5.8279(2)	5.431(3)
b (Å)	13.6150(4)	13.6150(4)	13.689(7)
c (Å)	5.8279(2)	6.3097(2)	5.892(3)
β (°)	111.760(2)	127.314(2)	111.79(4)
V (Å³)	398.19(3)	398.19(3)	406.7
Z	2		2
ρ_{calc} (g/cm³)	5.36		4.97
λ (Å)	0.71073		
μ (mm⁻¹)	34.08		
2θ range for data collection	≤70.11		
No. of reflections collected	8266		
No. of independent reflections	1798		
No. of reflections with $I > 2\sigma(I)$	1594		
No. of parameters refined	85		
R_{int}	0.029		
Final $R1$, $wR2$ factors [$I > 2\sigma(I)$]	0.023, 0.043		
Final $R1$, $wR2$ factors (all data)	0.028, 0.045		
Goodness-of-fit	1.024		

Note: The matrix for the transformation from setting I to II is (0 0 –1/0 1 0/1 0 1).

TABLE 3. Selected bond distances and angles in bartelkeite

	Distance (Å)		Distance (Å)
Pb-O1	2.703(3)	Fe-O3	2.043(2) x2
Pb-O2	2.645(2) x2	Fe-O4	2.213(2) x2
Pb-O3	2.473(2) x2	Fe-O5H	2.133(2) x2
Pb-O4	3.152(4) x2		
Pb-O6w	2.622(4)	Avg.	2.130
Pb-O6w	3.237(4)	OQE	1.042
		OAV	136.4
Avg.	2.789		
Ge1-O2	1.915(2) x2	Ge2-O1	1.754(1)
Ge1-O4	1.902(2) x2	Ge2-O2	1.734(2)
Ge1-O5H	1.849(2) x2	Ge2-O3	1.729(2)
		Ge2-O4	1.757(2)
Avg.	1.889	Avg.	1.744
OQE	1.004	TQE	1.007
OAV	11.4	TAV	26.8
O5H-H1	0.77(4)	O6w-H2	0.81(4)
O3···H1	2.02(4)	O5H···H2	2.03(4)
O5H···O3	2.761(3)	O6w···O5H	2.777(3)
∠O5H-H1-O3	160(5)°	∠O6w-H2-O5H	152(5)°

TABLE 2. Coordinates and displacement parameters of atoms in bartelkeite

Atom	*x*	*y*	*z*	U_{eq}	U_{11}	U_{22}	U_{33}	U_{23}	U_{13}	U_{12}
Pb	0.32486(4)	0.75	0.67674(3)	0.0149(1)	0.0142(1)	0.0155(1)	0.01618(8)	0	0.00984(7)	0
Fe	0.5	0	0	0.0077(1)	0.0082(3)	0.0087(3)	0.0066(2)	–0.0011(2)	0.0047(2)	–0.0016(2)
Ge1	0.5	0	0.5	0.0077(1)	0.0076(2)	0.0100(3)	0.0055(2)	0.0018(1)	0.0040(2)	0.0028(1)
Ge2	0.96137(6)	0.12998(3)	0.99604(6)	0.0069(1)	0.0058(1)	0.0072(2)	0.0065(1)	0.0001(1)	0.0032(1)	0.0005(1)
O1	0.9013(7)	0.75	0.9350(7)	0.0157(7)	0.011(1)	0.006(2)	0.027(2)	0	0.009(1)	0
O2	0.7512(5)	0.1115(2)	0.6545(4)	0.0128(5)	0.012(1)	0.015(1)	0.0084(9)	–0.0001(8)	0.0044(8)	–0.0031(8)
O3	0.7820(5)	0.3853(2)	0.1337(4)	0.0114(4)	0.013(1)	0.012(1)	0.0132(9)	0.0041(8)	0.0097(8)	0.0040(8)
O4	0.2838(4)	0.0625(2)	0.1610(4)	0.0088(4)	0.0083(9)	0.012(1)	0.0063(8)	0.0032(8)	0.0044(7)	0.0053(7)
O5H	0.2893(5)	0.0525(2)	0.6036(4)	0.0116(5)	0.0087(9)	0.018(1)	0.0074(8)	0.0017(8)	0.0046(7)	0.0037(8)
O6W	0.7617(9)	0.75	0.3216(8)	0.0240(8)	0.028(2)	0.012(2)	0.033(2)	0	0.019(2)	0
H1	0.143(6)	0.078(4)	0.495(7)	0.03*						
H2	0.713(8)	0.798(2)	0.355(9)	0.03*						

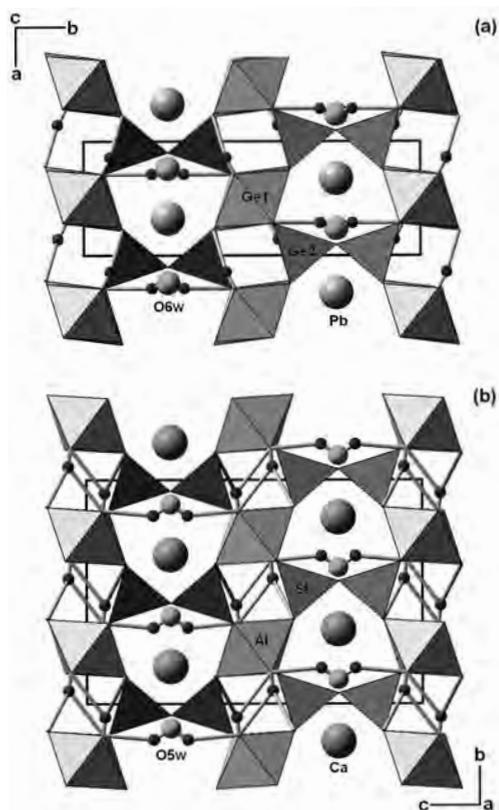* U_{iso} fixed during refinement.

FIGURE 1. Comparison of crystal structures of (**a**) bartelkeite and (**b**) lawsonite at 295 K (Libowitzky and Armbruster 1995). The FeO_6 octahedra in bartelkeite are beneath the $Ge1O_6$ octahedra. The large, medium, and small spheres represent Pb, O6w, and H atoms, respectively, in bartelkeite, and Ca, O5w, and H atoms in lawsonite.

edges to form single chains (Angel et al. 1988; Yang et al. 2009) and the O-Mg-O angle subtending the shared edge is 69.5°.

The Pb^{2+} cation in bartelkeite, due probably to its lone-pair electron activities, displays a (6+3) coordination, with six Pb-O bond lengths shorter than 2.70 Å and three longer than 3.15 Å (Table 3). By comparison, Sr^{2+} in the isostructural $P2_1/m$ itoigawaite, $SrAl_2Si_2O_7(OH)_2 \cdot H_2O$, is also 9-coordinated, but with all Sr-O bond distances falling between 2.53 and 2.93 Å (Liebscher et al. 2010), despite its similar size to Pb^{2+} ($R_{Pb^{2+}}$ = 1.29 Å and $R_{Sr^{2+}}$ = 1.31 Å) (Shannon 1976). Likewise, Pb^{2+} in synthetic *Pbnm* Pb-lawsonite, $PbAl_2Si_2O_7(OH)_2 \cdot H_2O$, can also be considered 9-coordinated, with the Pb-O bond distances ranging from 2.48 to 3.11 Å (Dörsam et al. 2011).

Contrary to the work by Keller et al. (1981), our structure analysis clearly indicates the presence of both OH and H_2O in bartelkeite, as shown by our bond-valence calculations using the parameters given by Brese and O'Keeffe (1991) (Table 4), as well as by our Raman spectroscopic measurements (see below). The hydrogen bonding scheme in bartelkeite (Table 3) is similar to that in lawsonite. However, OH in bartelkeite appears to be engaged in only one hydrogen bond, but two in lawsonite (Fig. 1).

Raman spectra

The Raman spectrum of bartelkeite is plotted in Figure 2. Based on previous Raman spectroscopic studies on various ger-

TABLE 4. Bond-valence sums for bartelkeite

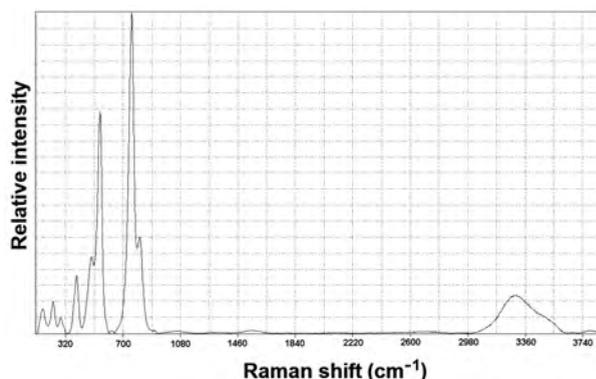|	Pb	Fe	Ge1	Ge2	ΣO
O1	0.20	—	—	$^{2\rightarrow\times}$ 0.98	**2.16**
O2	$^{2\downarrow\times}$ 0.24	—	$^{2\downarrow\times}$ 0.63	1.04	**1.91**
O3	$^{2\downarrow\times}$ 0.38	$^{2\downarrow\times}$ 0.43	—	1.05	**1.86**
O4	$^{2\downarrow\times}$ 0.06	$^{2\downarrow\times}$ 0.27	$^{2\downarrow\times}$ 0.66	0.97	**1.96**
O5H	—	$^{2\downarrow\times}$ 0.34	$^{2\downarrow\times}$ 0.76	—	**1.10**
O6W	0.25				
	0.05	—	—	—	**0.30**
ΣM	**1.86**	**2.08**	**4.10**	**4.04**	

FIGURE 2. Raman spectrum of bartelkeite.

manate materials (e.g., Ross et al. 1986; Baran et al. 2004; Takahashi et al. 2008), we made the following tentative assignments for the major bands. The two broad bands at 3293 and 3490 cm^{-1} are due to O-H stretching vibrations. According to Libowitsky (1999), these two bands correspond to estimated O···O distances of ~2.75 and 2.95 Å, respectively, which are compared to the O5H···O3 (2.76 Å) and O6w···O5H (2.78 Å) distances from the structure refinement (Table 3). The very weak and broad band at 1558 cm^{-1} is characteristic of the H-O-H bending vibration. The two bands at 758 (the strongest) and 812 cm^{-1} are attributed to the symmetric and antisymmetric stretching vibrations of Ge-O bonds within the GeO_4 tetrahedron, respectively, whereas the band at 492 cm^{-1} is assigned to the Ge-O stretching vibrations within the GeO_6 octahedron. The two bands at 549 (the second strongest) and 393 cm^{-1} are ascribed to the Ge^{IV}-O-Ge^{IV} and Ge^{VI}-O-Ge^{IV} bending vibrations, respectively. The bands below 320 cm^{-1} are of complex nature and mostly associated with the rotational and translational modes of GeO_4 and GeO_6 polyhedra, Fe-O interactions, and the lattice vibrational modes.

Implications for lawsonite

Lawsonite is an index mineral for high-pressure low-temperature metamorphism (such as blueschist facies). Its high-H_2O content (11.5 wt%) and high-pressure stability, up to ~12 GPa at 1240 K, make it a potential host for water in subducting slabs down to as much as 250 km (Pawley 1994; Schmidt 1995). Recent experimental studies have uncovered the intricate behavior of this mineral as a function of temperature, pressure, and composition. On the one hand, lawsonite undergoes two reversible phase transitions attributed to the order-disorder of hydrogen bonding at low temperatures, one from *Cmcm* to *Pmcn* at 273 K and the other from *Pmcn* to $P2_1cn$ at 155 K (Libowitzky and Armbruster

1995; Meyer et al. 2001; Sondergeld et al. 2005; Kolesov et al. 2008 and references therein). On the other hand, it exhibits an unquenchable, displacive transition from *Cmcm* to *P*2$_1$/*m* at high pressures above 8.6 GPa (Daniel et al. 2000; Pawley and Allan 2001; Boffa Ballaran and Angel 2003). However, the stability field of this high-pressure *P*2$_1$/*m* phase is still undefined. In addition, Liebscher et al. (2010) noticed a *Cmcm*-to-*P*2$_1$/*m* symmetry change as the substitution of Sr for Ca increases in lawsonite, whereas Dörsam et al. (2011) synthesized *Pbnm* Pb-lawsonite, $PbAl_2Si_2O_7(OH)_2 \cdot H_2O$ at 2 GPa and 600 °C. The determination of the bartelkeite structure implies that the lawsonite- or bartelkeite-type structure or topologically similar structures can be rather compliant and complex, and a variety of such compounds with different cation sizes and valences may be synthesized or found in nature, such as $CaMgSi^{VI}(Si_2O_7)(OH)_2 \cdot H_2O$, $NaAlSi^{VI}(SiO_7)$ $(OH)_2 \cdot H_2O$, $CaAlCr(Si_2O_7)(OH)_2 \cdot H_2O$, and $BaFeTi(Si_2O_7)$ $(OH)_2 \cdot H_2O$. Furthermore, it suggests that bartelkeite-type compounds can serve as good models for further exploration of the temperature-pressure-composition space of lawsonite and the discovery of more exotic phases at various temperatures and pressures.

REFERENCES CITED

Angel, R.J., Gasparik, T., Ross, N.L., Finger, L.W., Prewitt, C.T., and Hazen, R.M. (1988) A silica-rich sodium pyroxene phase with six-coordinated silicon. Nature, 335, 156–158.

Baran, E.J., Mercader, R.C., and Cascales, C. (2004) Vibrational and ^{57}Fe-Mössbauer spectra of $LaFeGe_2O_7$ and $NdFeGe_2O_7$. Journal of Physics and Chemistry of Solids, 65, 1913–1915.

Boffa Ballaran, T. and Angel, R.J. (2003) Equation of state and high-pressure phase transitions in lawsonite. European Journal of Mineralogy, 15, 241–246.

Brese, N.E. and O'Keeffe, M. (1991) Bond-valence parameters for solids. Acta Crystallographica, B47, 192–197.

Daniel, I., Fiquet, G., Gillet, P., Schmidt, M.W., and Hanfland, M. (2000) High-pressure behavior of lawsonite: a phase transition at 8.6 GPa. European Journal of Mineralogy, 21, 721–733.

Dörsam, G., Liebscher, A., Wunder, B., Franz, G., and Gottschalk, M. (2011) Synthesis of Pb-zoisite and Pb-lawsonite. Neues Jahrbuch für Mineralogie, Abhandlungen, 188, 99–110.

Frost, D.J. (2006) The stability of hydrous mantle phases. In H. Keppler and J.R. Smyth, Eds., Water in Nominally Anhydrous Minerals, 62, p. 243–271. Reviews in Mineralogy and Geochemistry, Mineralogical Society of America, Chantilly, Virginia.

Hazen, R.M., Downs, R.T., and Finger, L.W. (1996) High-pressure framework silicates. Science, 272, 1769–1771.

Henderson, G.S. and Wang, H.M. (2002) Germanium coordination and the germanate anomaly. European Journal of Mineralogy, 14, 733–744.

Iezzi, G., Boffa Ballaran, T., McCammon, C., and Langenhorst, F. (2005) The $CaGeO_3$–$Ca_3Fe_2Ge_3O_{12}$ garnet join: an experimental study. Physics and Chemistry of Minerals, 32, 197–207.

Keller, P., Hess, H., and Dunn, P., and Bartelkeit, J. (1981) PbFe^{2+}Ge$_3$O$_8$, ein neues Germanium-Mineral von Tsumeb, Namibia. Chemie der Erde, 40, 201–206.

Kolesov, B.A., Lager, G.A., and Schultz, A.J. (2008) Behaviour of H_2O and OH in lawsonite: a single-crystal neutron diffraction study and Raman spectroscopic investigation. European Journal of Mineralogy, 20, 63–72.

Libowitsky, E. (1999) Correlation of O–H stretching frequencies and O–H.O hydrogen bond lengths in minerals. Monatshefte für Chemie, 130, 1047–1059.

Libowitzky, E. and Armbruster, T. (1995) Low-temperature phase transitions and the role of hydrogen bonds in lawsonite. American Mineralogist, 80, 1277–1285.

Liebscher, A., Dörsam, G., Franz, G., Wunder, B., and Gottschalk, M. (2010) Crystal chemistry of synthetic lawsonite solid-solution series $CaAl_2[(OH)_2/Si_2O_7] \cdot H_2O$-$SrAl_2[(OH)_2/Si_2O_7] \cdot H_2O$ and the *Cmcm*-*P*2$_1$/*m* phase transition. American Mineralogist, 95, 724–735.

Meyer, H-W., Marion, S., Carpenter, M.A., Knight, K.S., Redfern, S.A.T., and Dove, M.T. (2001) Displacive components of the low temperature phase transitions in lawsonite. American Mineralogist, 86, 566–577.

Nestola, F., Németh, P., Angel, R.J., and Buseck, P.R. (2008) Equation of state and crystal structure of a new germanate post-titanite phase. American Mineralogist, 93, 1424–1428.

Pawley, A.R. (1994) The pressure and temperature stability limits of lawsonite: Implications for H_2O recycling in subduction zones. Contributions to Mineralogy and Petrology, 118, 99–108.

Pawley, A.R. and Allan, D.R. (2001) A high-pressure structural study of lawsonite using angle-dispersive powder-diffraction methods with synchrotron radiation. Mineralogical Magazine, 65, 41–58.

Ringwood, A.E. and Major, A. (1967) High-pressure reconnaissance investigations in the system Mg_2SiO_4-MgO-H_2O. Earth and Planetary Science Letters, 2, 130–133.

Ringwood, A.E. and Seabrook, M. (1963) High-pressure phase transitions in germanate pyroxenes and related compounds. Journal of Geophysical Research, 68, 4601–4609.

Robinson, K., Gibbs, G.V., and Ribbe, P.H. (1971) Quadratic elongation: a quantitative measure of distortion in coordination polyhedra. Science, 172, 567–570.

Ross, N.L., Akaogi, M., Navrotsky, A., Susaki, J.I., and McMillan, P. (1986) Phase transitions among the $CaGeO_3$ polymorphs (wollastonite, garnet and perovskite structures): studies by high-pressure synthesis, high-temperature calorimetry, and vibrational spectroscopy and calculation. Journal of Geophysical Research, 91, 4685–4696.

Schmidt, M.W. (1995) Lawsonite: upper pressure stability and formation of higher density hydrous phases. American Mineralogist, 80, 1286–1292.

Shannon, R.D. (1976) Revised effective ionic radii and systematic studies of interatomic distances in halides and chalcogenides. Acta Crystallographica, A32, 751–767.

Sheldrick, G.M. (2008) A short history of *SHELX*. Acta Crystallographica, A64, 112–122.

Sondergeld, P., Schranz, W., Tröster, A., Armbruster, T., Giester, G., Kityk, A., and Carpenter, M.A. (2005) Ordering and elasticity associated with low-temperature phase transitions in lawsonite. American Mineralogist, 90, 448–456.

Takahashi, Y., Iwashaki, K., Masai, H., and Fujiwara, T. (2008) Raman spectroscopic study of benitoite-type compounds. Journal of the Ceramics Society of Japan, 116, 1139–1142.

Thomas, S-M., Müller, M.K., Kahlenberg, V., Thomas, B., Rhede, D., Wirth, R., and Wunder, B. (2008) Protonation in germanium equivalents of ringwoodite, anhydrous phase B, and superhydrous phase B. American Mineralogist, 93, 1282–1294.

Thompson, A.B. (1992) Water in the Earth's upper mantle. Nature, 358, 295–302.

Wunder, B. and Marler, B. (1997) Ge-analogues of aluminium silicates: High-pressure synthesis and properties of orthorhombic $Al_2GeO_4(OH)_2$. European Journal of Mineralogy, 9, 1147–1158.

Yang, H., Konzett, J., Frost, D.J., and Downs, R.T. (2009) X-ray diffraction and Raman spectroscopic studies of clinopyroxenes with six-coordinated Si in the $Na(Mg_{0.5}Si_{0.5})Si_2O_6$-$NaAlSi_2O_6$ system. American Mineralogist, 94, 942–949.